Dynamic Response of Pressure Sensing Systems in Slip-Flow with Temperature Gradients

Stephen A. Whitmore*
NASA Dryden Flight Research Center, Edwards, California 93523
and
Brian J. Petersen†
The Boeing Company, Long Beach, California 90013

Introduction

THE accurate sensing of surface pressures on hypersonic flight vehicles presents formidable measurement challenges. The hostility of the sensing environment precludes intrusion into the flow, and measurements must be obtained via sizable lengths of small-diameter pneumatic tubing that connect the surface ports to the remotely located pressure transducers. An idealized pneumatic layout is depicted in Fig. 1. Further complicating the sensing problem is surface boundary layer heating, which causes sizable temperature gradients within the pneumatic tubing. Away from the stagnation region, local surface pressure levels, which must be sensed, are extremely low, often less than 0.002 atmospheres (0.2 KPa). The combination of very low pressure levels, small diameter pneumatic lines, and large temperature gradients makes molecular effects no longer negligible.

The problem of predicting tube flow dynamics has been studied extensively. For nonrarefied conditions, Lamb,[1] Iberall,[2] Schuder and Binder,[3] and Hougen et al.,[4] have developed closed-form frequency domain solutions for simple tubing geometries and constant wall temperatures. Berg and Tijdeman[5] and Tijdeman[6] extended the analyses of Refs. 3 and 4 to develop a recursion formula for complex geometries that consist of cascades of tubes and volumes. Parrot and Zorumski[7] investigated the dynamic transmission of sound in a simple geometry tube subjected to very large temperature gradients. References 1–7 considered only continuum flow conditions; rarefied flow effects were not investigated. Tube flow for rarefied conditions at high temperatures with large temperature gradients has been investigated by Maxwell,[8] von Knudsen,[9] and Tompkins and Wheeler.[10] These rarefied flow investigations, however, considered only steady-flow conditions.

The dynamic influence of rarefied flow phenomena on pneumatic pressure sensing systems has not been generally well understood; consequently, research was initiated at the NASA Dryden Flight Research Center with a primary objective to develop a dynamic response model for pneumatic pressure sensing systems that is applicable to both continuum and rarefied flows. Whitmore et al.[11] presented a detailed analytical development and empirical validation of one such model. This Note summarizes the information presented in that text.

Mathematical Analysis

The model of Berg and Tijdeman[5,6] is extended to allow for rarefied conditions by modifying the wall boundary condition to allow fluid elements to "slip" and flow at the tube wall. This boundary condition contrasts to the classical "no-slip" condition used for continuum flow mechanics. "Slip-flow" conditions correspond to values of the Knudsen number that lie between 0.01 and 1.0. The Knudsen number is defined as the ratio of the molecular-mean free path distance λ, the average distance each fluid particle travels between collisions and the characteristic scale length of the system. If the scale length of the system is taken to be the tube radius R, the Knudsen number can be approximated by the expression[12]

$$\kappa \approx \sqrt{R_g \pi}(\mu/R)(\sqrt{T}/P) \tag{1}$$

where μ is the dynamic viscosity, R_g is the universal gas constant, T is the gas temperature, and P is the local pressure. For hypersonic and orbital applications, typical Knudsen number variations from 0.05 to 0.50 are experienced at high altitudes. Other than the wall boundary condition modification, the classical equations of fluid motion apply in the slip-flow regime.

For slip-flow conditions, the fluid velocity at the wall boundary can be decomposed into two parts: the thermomolecular "creep" velocity, and the slip-velocity.[12] The molecular creep velocity is proportional to the local longitudinal temperature gradient and inversely proportional to the local pressure. The slip-velocity is proportional to wall shearing stress. The modified wall boundary condition may be written as

$$U_{\text{wall}}(x,t) = U_{\text{creep}} + U_{\text{slip}} \approx \frac{3}{4}\frac{\mu_0 R_g}{\bar{P}_0}\frac{\partial T}{\partial x} - \vartheta\frac{\partial U}{\partial r} \tag{2}$$

where μ_0 and $\bar{P}_0$ are longitudinal averages of viscosity and pressure. The U is longitudinal velocity, r is the radial coordinate, and $\partial T/\partial x$ is the longitudinal temperature gradient.

In Eq. (2) the molecular creep is caused by gas molecules originating from the hot region of the tube having higher kinetic energy than molecules originating from the cold region. The result is that the hot-end molecules recoil from collisions more strongly, and the gas molecules at the wall acquire a net tangential momentum toward the hot end of the tube. To balance this wall-flow gas molecules near the center of the tube (away from the real-gas effects) migrate toward the colder end of the tube, with the result being no net cross-sectional flow in the tube. For high-Knudsen-number flows the wall creep-flow dominates, causing the pressure in the cold region of the tube to read lower than the pressure in the hot region. The parameter ϑ is an empirical factor defined as the slip distance, and accounts for the reduced fluid viscosity under rarefied flow conditions. The ratio of slip distance to the mean free path, $k_{\text{ratio}} = \vartheta/\lambda$, for various materials and gases are tabulated by Kennard.[12] For conventional metals k_{ratio} is approximately unity. For ceramic materials such as quartz glass, k_{ratio} is approximately 1.25.

Following the procedure laid out by Berg and Tijdeman,[5,6] the equations of motion are linearized using small perturbations, and the energy equation is decoupled from the momentum and continuity equations by assuming that the wave expansion process in the tube is polytropic, a simple energy model that relates pressure, temperature, and density[13,14]:

$$P = K\rho^{\xi} \tag{3}$$

The polytropic expansion parameter ξ has limiting values given by $1 < \xi < \gamma$, where γ is the ratio of specific heats. Values of $\xi = 1$ correspond to an irreversible expansion, and $\xi = \gamma$ corresponds to an isentropic expansion. The boundary value equations are radially averaged and solved assuming gas properties remain constant along the length of the tube. This fundamental solution is used as a building block for complex solutions where fluid properties and tubing geometry may vary longitudinally. The problem is solved recursively assuming n solution nodes starting at the transducer end (nth node) and working toward the surface end (0th node) of the tube. Using the recursive formulas, solutions for arbitrary geometries and longitudinal temperature profiles are constructed. The resulting recursive formula for the frequency response of the pressure sensor is

$$\frac{P_L(\omega)}{P_0(\omega)} = \frac{P_1(\omega)}{P_0(\omega)}\frac{P_2(\omega)}{P_1(\omega)}\cdots\frac{P_{n-1}(\omega)}{P_{n-2}(\omega)}\frac{P_n(\omega)}{P_{n-1}(\omega)} =$$

$$\prod_{i=1}^{n}\frac{1}{\cosh\left[\omega\Gamma_{p_i}L_i/c_i\right] + \omega\left(V_{e_i}\Gamma_{p_i}\right)/\left(A_{c_i}c_i\right)\sinh\left[\omega\Gamma_{p_i}L_i/c_i\right]} \tag{4}$$

Received Feb. 11, 1998; revision received Jan. 20, 1999; accepted for publication Feb. 8, 1999.

*Vehicle Aerodynamics Group Leader, Aerodynamics Branch. Senior Member AIAA.
†Aerospace Engineer, Douglas Aircraft Division. Member AIAA.

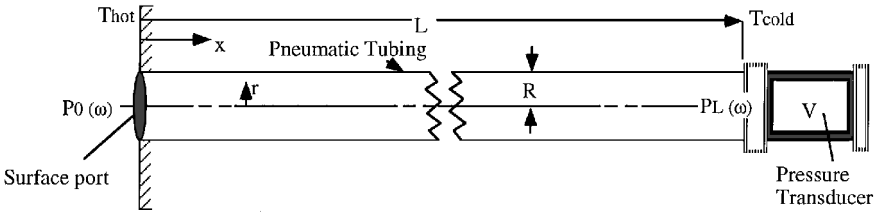

Fig. 1 Idealized schematic of pressure sensor configuration.

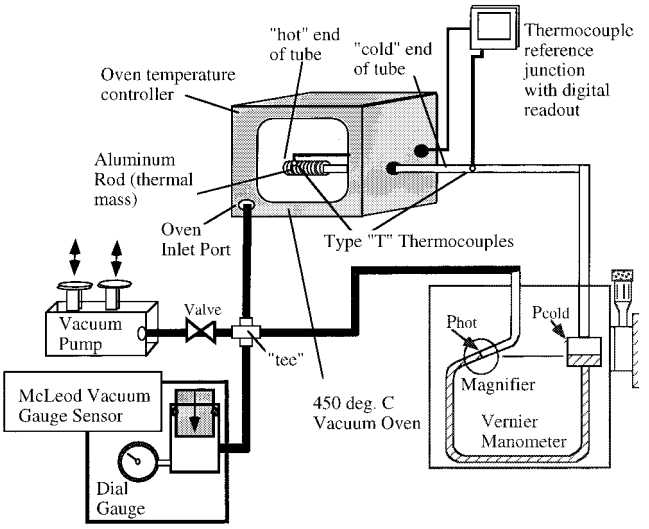

Fig. 2 Schematic of experimental apparatus.

where the parameter V_e is the effective volume and accounts for the entrapped volume at the ith node plus the impedance of the downstream tubes and volumes:

$$V_{e_i} = V_i \left\{ 1 + \frac{\left(c_i^2 / c_{i+1}^2\right)\left(V_{e_{i+1}} / V_i\right)\left[\cosh\left[\omega\Gamma_{p_{i+1}}(L_{i+1}/c_{i+1})\right]\right] + \left[1/\omega\left(V_{e_{i+1}}/A_{c_{i+1}}\right)\left(\Gamma_{p_{i+1}}/c_{i+1}\right)\right]\sinh\left[\omega\Gamma_{p_{i+1}}(L_{i+1}/c_{i+1})\right]\right]}{\cosh\left[\omega\Gamma_{p_{i+1}}(L_{i+1}/c_{i+1})\right] + \omega\left(V_{e_{i+1}}/A_{c_{i+1}}\right)\left(\Gamma_{p_{i+1}}/c_{i+1}\right)\sinh\left[\omega\Gamma_{p_{i+1}}(L_{i+1}/c_{i+1})\right]} \right\} \tag{5}$$

The parameter Γ_p is referred to as the wave propagation factor[5,6,11] and is evaluated by

$$\Gamma_p \equiv \sqrt{\frac{\gamma}{\xi}\frac{J_0[\alpha] - \vartheta(\alpha/R)J_1[\alpha]}{\left\{\kappa_p\left(J_2[\alpha] + \vartheta(\alpha/R)J_1[\alpha]\right) + j\omega\frac{3}{4}(\mu/\bar{P}_0)[(\xi-1)/\xi](2/\alpha)J_1[\alpha]\right\}}} \tag{6}$$

As developed by Berg and Tijdeman,[5,6] the variation of ξ as a function of the fundamental flow parameters is given by

$$\xi = \left[1 + \left[\frac{\gamma - 1}{\gamma}\right]\frac{J_2[\sqrt{Pr}\alpha]}{J_0[\sqrt{Pr}\alpha]}\right]^{-1} \tag{7}$$

In Eqs. (4–7) the symbol definitions are $j = \sqrt{-1}$, c = sonic velocity, A_c = tube cross-sectional area, P_L = pressure at transducer, ρ_0 = longitudinally averaged density in tube, $\kappa_p = 1 + 4j\omega\mu/(3\xi\bar{P}_0)$ = rarefied flow correction factor for the bulk viscosity, ω = radian frequency of unsteady input pressure, $\alpha \equiv j^{3/2}\sqrt{(\omega\rho_0 R^2/\mu_0)}$ = shear wave number, J_0 = zeroth-order Bessel function, J_1 = first-order Bessel function, J_2 = second-order Bessel function, and Pr = Prantl number. At the nth node, V_n = the volume entrapped by the pressure transducer. If the rarefied flow terms are dropped from Eqs. (4–7), then the algorithm reduces exactly to the recursion model developed for continuum flow by Berg and Tijdeman.[5,6] As mentioned previously, Whitmore et al.[11] presented a detailed derivation of Eqs. (4–7) and an extensive dynamic validation of the model for continuum flow conditions with large temperature gradients.

Model Validation

The steady-state behavior of the dynamic model was analyzed by applying the final value theorem[15] to Eqs. (4–7). The resulting expression is nondimensionalized and written as a function of the longitudinally averaged Knudsen number κ_0:

$$\left(\frac{\partial P}{\partial x}\Big/ P\right) = \left(\frac{\partial T}{\partial x}\Big/ T\right)\frac{6\kappa_0^2}{\pi(1 + 4k\kappa_0)} \tag{8}$$

In Eq. (8), $\partial P/\partial x$ and $\partial T/\partial x$ are the longitudinal pressure and temperature gradients in the tube. Because it is impractical conduct controlled frequency response experiments for rarefied conditions, the steady-state analysis is extremely important because it is the best available means of evaluating the validity range of the dynamic model presented in Eqs. (4–7).

A series of steady-state laboratory tests were conducted to determine the upper limit of κ_0 for which the model is valid. The test apparatus is depicted in Fig. 2. Tests were performed in an evacuated vacuum oven. Here, aluminum rods were bored with holes, and an assortment of brass tubes of varying diameters and lengths was press-fit into the holes. The aluminum rods provided a thermal mass to distribute the heat evenly along one end of the tubing. Thermocouples bonded to each end of the tube were used to sense temperatures and the temperature gradient along the tube. The cold end of the tube was hermetically bonded to a compression fitting that allowed the heated tube to be accessed from outside the chamber. The chamber pressure was measured using a McLeod vacuum gauge[16] and the differential pressure in the heated tube was measured using a highly sensitive Vernier manometer.[16]

The oven proved sufficient to allow temperature gradients as high as 1340°C/cm, and chamber pressures as low as 100 μm of mercury (0.013 kPa). The resulting values for κ_0 varied from near zero to approximately 10.0. Dividing the normalized pressure differential in the tube by the normalized temperature differential, the data was collapsed into a single curve by plotting the result as a function κ_0. These data are plotted in Fig. 3 along with the model steady-state predictions. Comparisons are good for κ_0 up to approximately 0.65. For $\kappa_0 > 0.65$ free molecule effects dominate and the model rapidly diverges from the data. This divergence point marks the upper bound on the model's usefulness. Fortunately, it appears that the model is valid for most of the slip-flow regime.

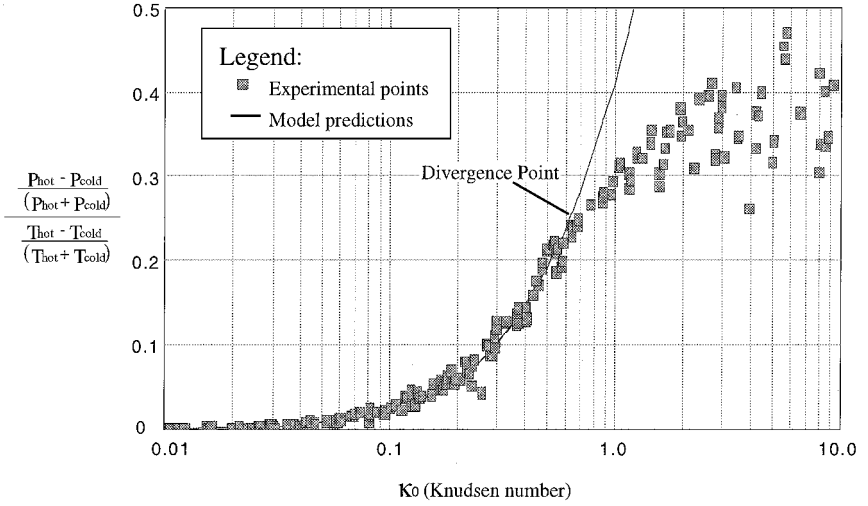

Fig. 3 Comparison of the steady-state model response to experimental results.

Conclusion

This Note reports on the development of a dynamic model for pressure sensing configurations in high Knudsen number flows. The model, applicable to both continuum and rarefied flow conditions, allows for longitudinal temperature gradients in the sensor configuration. The applicable flow regimes for the model were evaluated by a series laboratory tests. Model comparisons are excellent for Knudsen numbers up to 0.65. For values of $\kappa_0 > 0.65$, free molecule effects dominate, and the model is no longer valid. The model represents a fundamental contribution to the understanding of flow behavior at the limits of the continuum flow regime. The model allows instrumentation designers to evaluate the responses of pneumatic systems over a wide range of flow conditions that may vary continuously from continuum to slip-flow. Other potential applications outside of aerospace include predicting the behavior of micromachined fluid systems where the mean free path of the working fluid is on the order of the channel diameter.

References

[1]Lamb, R. C., "The Influence of Geometry Parameters upon Lag Error in Airborne Pressure Measurement Systems," Wright Air Development Center, TR 57-351, Wright–Patterson AFB, OH, July 1957.

[2]Iberall, A. S., "Attenuation of Oscillatory Pressures in Instrument Lines," U.S. National Bureau of Standards, Rept. RP 2115, Vol. 45, Washington, DC, July 1950.

[3]Schuder, C. B., and Binder, R. C., "Response of Pneumatic Transmission Lines to Step Inputs," *Journal of Basic Engineering*, Vol. 81, No. 12, 1959, pp. 578–584.

[4]Hougen, J. O., Martin, O. R., and Walsh, R. A., "Dynamics of Pneumatic Transmission Lines," *Journal of Control Engineering*, Vol. 10, No. 3, 1963, pp. 114–117.

[5]Berg, H., and Tijdeman, H., "Theoretical and Experimental Results for the Dynamic Response of Pressure Measuring Systems," Nat. Luchtavaatlab, NLR-TR F.238, Amsterdam, The Netherlands, Jan. 1965.

[6]Tijdeman, H., "Investigation of the Transonic Flow Around Oscillating Airfoils," Nat. Luchtavaatlab, NLR-TR 77090 U, Amsterdam, The Netherlands, Sept. 1977.

[7]Parrot, T. L., and Zorumski, W., "Sound Transmission Through a High-Temperature Acoustic Probe Tube," *AIAA Journal*, Vol. 30, No. 2, 1992, pp. 318–323.

[8]Maxwell, J. C., "On Stress in Rarefied Gases Arising from Inequalities of Temperature," *Journal of Philosophical Transactions*, Vol. 170, Pt. 1, 1879, pp. 231–235.

[9]von Knudsen, M., "Eine Revision der Gleichgewichtsbedingung der Gase: Thermische Molekularströmung," *Annalen dek Physik*, Vol. 31, Nov. 1910, pp. 205–229.

[10]Tompkins, J., and Wheeler, L., "The Correction for Thermo-Molecular Flow," *Transactions of the Faraday Society*, Vol. 29, Nov. 1933, pp. 1248–1254.

[11]Whitmore, S. A., Petersen, B. J., and Scott, D. D., "A Dynamic Response Model for Pressure Sensors in Continuum and High Knudsen Number Flows with Large Temperature Gradients," NASA TM-4728, Jan. 1996.

[12]Kennard, E. H., *Kinetic Theory of Gases*, McGraw–Hill, New York, 1938, pp. 311–337.

[13]Stephens, R. W. B., and Bate, A. E., *Acoustics and Vibrational Physics*, St. Martin, New York, 1966, pp. 660–682.

[14]Freiberger, W. F. (ed.), *The International Dictionary of Applied Mathematics*, Van Nostrand, Princeton, NJ, 1960, p. 707.

[15]Rade, L., and Westergren, B., *Beta Mathematics Handbook*, CRC Press, Boca Raton, FL, 1994, pp. 287–288.

[16]Doeblin, E. O., *Measurement Systems Application and Design*, McGraw–Hill, New York, 1983, pp. 410–455.

R.P. Lucht
Associate Editor

Postbuckling of Delaminated Composites Under Compressive Loads Using Global–Local Approach

Jun-Sik Kim* and Maenghyo Cho†
Inha University, Inchon 402-751, Republic of Korea

I. Introduction

To describe the damage process of delaminated composites up to final failure, bifurcation buckling analysis might not be enough, and a postbuckling analysis may be required because composite laminates have load-carrying capacity above the buckling loads. Three-dimensional elasticity models[1] or layerwise plate models[2] are adequate to predict postbuckling behaviors of multiple delaminated composite laminates. However, these kinds of analyses require large amounts of computer resources. Thus, for an engineering analysis to save computing time and memory, a global–local analysis is a suitable choice for compromising accuracy and efficiency. However, the postbuckling problems for the laminates with multiple delaminations are not reported in the global–local approaches.

The failure analysis of delaminated plates is quite complicated because it includes postbuckling load increments, iterations of delamination zone propagation, and a contact algorithm between delaminated interfaces. Thus, the numerical analysis of a failure mechanism involves multistep nonlinear iterations. To treat this whole

Received Aug. 10, 1996; presented as Paper 97-1293 at the AIAA/ASME/ASCE/AHS/ASC 38th Structures, Structural Dynamics, and Materials Conference, Kissimmee, FL, April 7–10, 1997; revision received Oct. 20, 1998; accepted for publication Feb. 5, 1999.

*Graduate Research Assistant, Department of Aerospace Engineering, 253 Yong-Hyun Dong Nam-Ku.

†Assistant Professor, Department of Aerospace Engineering, 253 Yong-Hyun Dong Nam-Ku. Member AIAA.